Theoretically Identified Strong Coupling of Carbonation Rate and Thermodynamic Moisture States in Micropores of Concrete

Tetsuya Ishida[1], Koichi Maekawa[2] and Masoud Soltani[3]

Received 4 December 2003, accepted 6 April 2004

Abstract

In order to predict the chemo-physical process of carbonation, a finite element based computational method is implemented based upon multi-phase/scale governing equations of moisture and flux of both heat and carbon dioxide. Influencing parameters of carbonation involving reaction rate, CO_2 diffusivity and the reduction of porosity are discussed. It is found that such modeling can accurately show high nonlinearity among carbonation reaction, pore structure development and moisture distribution in micropore structures. By using the proposed assumptions, the reliability of the predictive method of the carbonation mechanism in cementitious materials under arbitrary environmental and curing conditions is examined by comparing available experimental results with theoretical ones. Through sensitivity analyses that focus on the nonlinearity of the moisture profile and local carbonation, it is clarified that different moisture distribution may bring the opposite trend of the carbonation depth under low and high CO_2 concentrations.

1. Introduction

One of the main factors controlling the serviceability and safety performance of structural concrete is the corrosion of steel reinforcing bars. The passive layer around the steel bars naturally protects them from corrosion. However, the penetration of carbon dioxide and the consumption of calcium hydroxide may cause a drop in the pH value of the pore water. Under low pH conditions, the thin oxide film around the steel surface breaks down and its ability to protect the steel bars from corrosion declines.

Reliable prediction of long-term performance of structural concrete requires accurate and versatile simulation of chemophysical phenomena for arbitrary environmental conditions and concrete characteristics. Mathematical expressions of concrete deterioration employ strong coupling mechanisms of hydration, moisture transport, pore-structure development (early-age characteristics) and the long-term qualities of concrete. In this paper, a three-dimensional finite element program, *DuCOM*, developed at the University of Tokyo, is implemented as a general framework for durability assessment and numerical analysis of arbitrary cementitious materials and structures subjected to various environmental conditions. A general framework of mass and ion equilibrium equations and a chemical reaction model of carbonation in micropore spaces have been presented elsewhere in detail (Maekawa *et al*. 1999, 2002, 2003, Ishida and Maekawa 2001). Thus the influential parameters on theorem of carbonation process are discussed and simulated in numerical terms in this paper. The reliability of the model is verified through comparison of simulation with well-documented experimental results. Here, the dissimilarity of carbonation depth under dense CO_2 in an acceleration chamber and natural ambient conditions is theoretically explained and faithfully simulated in nature.

2. General thermo-hygro system *DuCOM*

The constituent material models employed in *DuCOM* are formulated based on micro-mechanical phenomena such as hydration, moisture transport and cementitious microstructure formation (Maekawa *et al*. 1999, 2003). Their strong interrelationships are taken into account by real-time sharing of material characteristic variables across each sub-system. The development of multi-scale micro pore structures at early ages is obtained based on the average degree of cement hydration in the mixture. For any arbitrary initial and boundary conditions, the pore pressure, relative humidity and moisture distribution are mathematically simulated according to a moisture transport model that considers both vapor and liquid modes of mass transport.

The moisture distribution, relative humidity and micropore structure characteristics in turn control the carbon-dioxide diffusion, reaction and the rate of carbonation under arbitrary environmental conditions. This nonlinearity problem and coupling terms can be taken into account in the unified framework of the program as schematically shown in **Fig. 1**.

[1]Associate Professor, Department of Civil Engineering, University of Tokyo, Japan
E-mail: tetsuya.ishida@civil.t.u-tokyo.ac.jp
[2]Professor, Department of Civil Engineering, University of Tokyo, Japan
[3]Assistant Professor, Department of Civil Engineering, Tarbiat Modares University, Iran

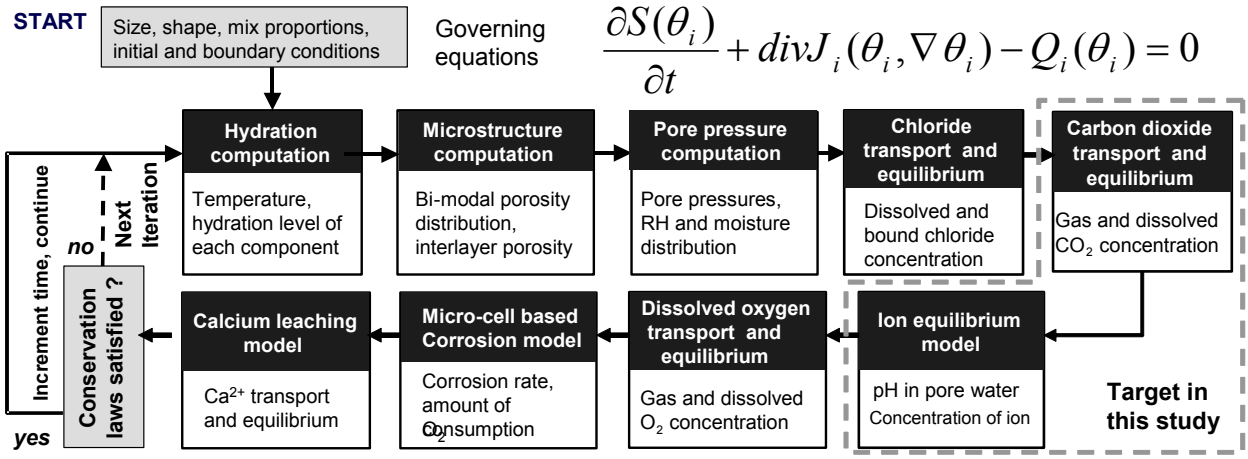

Degree of freedom: temperature, pore liquid pressure, concentrations of free chloride, carbon dioxide, oxide, calcium ion

Fig. 1 Overall scheme of *DuCOM* thermo-hygro coupled system.

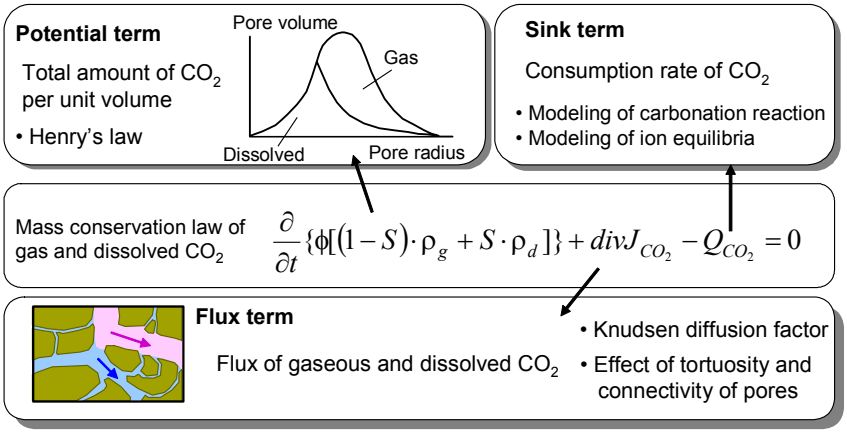

Fig. 2 Governing equation and constituting models.

3. Carbon dioxide transport, equilibrium, reaction model

The mass balance equation for a porous medium, which expresses the equilibrium of the concentration of gaseous and dissolved carbon dioxide within the time and space domains, is formulated as,

$$\frac{\partial}{\partial t}\left\{\phi\left[(1-S)\rho_g + S\rho_d\right]\right\} + divJ_{CO2} - Q_{CO2} = 0 \qquad (1)$$

where, ϕ = porosity, S = saturation of porosity, ρ_g = density of gaseous carbon dioxide[kg/m^3], ρ_d = density of dissolved carbon dioxide in pore water [kg/m^3], and J_{CO2} = total flux of dissolved and gaseous carbon dioxide [kg/m^{2}s]. Equation (1) represents the equilibrium condition between rates of mass efflux from a control volume, mass flow into the control volume and accumulation of mass within the control volume. The above equation gives the concentrations of gaseous and dissolved carbon dioxide with time and space. The governing equation (1) is simultaneously associated with the moisture analysis scheme in terms of the saturation denoted by S and other thermodynamic parameters used in the flux term as shown in **Fig. 2**. The moisture computation details are available in the references (Maekawa *et al*. 1999, 2003) and are not covered in this paper.

The local equilibrium of gaseous and dissolved carbon dioxide is represented by Henry's law (Ishida and Maekawa 2001). The rate of carbon dioxide consumption is expressed by the following differential equation, assuming that the reaction is of the first order with respect to the Ca^{2+} and CO_3^{2-} concentrations as,

$$Q_{CO2} = \frac{\partial(C_{CaCO_3})}{\partial t} = k[Ca^{2+}][CO_3^{2-}] \qquad (2)$$

where, C_{CaCO3} = concentration of calcium carbonate [mol/l], and k = reaction rate coefficient [l/mol.sec]. The concentration of calcium carbonate per unit time obtained by the above equation is equal to the consumption rate of carbonic acid, which is the sink term Q_{CO2} in mass balance equation (1). In order to calculate the rate of reaction with Eq. (2), it is necessary to obtain the

concentration of calcium ion and carbonic acid in the pore water at an arbitrary stage. In this model, we consider the following ion equilibriums: dissociation of water and carbonic acid, and dissolution and dissociation of calcium hydroxide and calcium carbonate (see **Fig. 3**).

$$\begin{aligned} &H_2O \leftrightarrow H^+ + OH^- \\ &H_2CO_3 \leftrightarrow H^+ + HCO_3^- \leftrightarrow 2H^+ + CO_3^{2-} \\ &Ca(OH)_2 \leftrightarrow Ca^{2+} + 2OH^- \\ &CaCO_3 \leftrightarrow Ca^{2+} + CO_3^{2-} \end{aligned} \tag{3}$$

Ishida and Maekawa (2001) introduced a governing equation with respect to the concentration of proton $[H^+]$, based on the laws of mass action, mass conservation and proton balance which can be iteratively solved in order to obtain the concentration of proton in pore solutions at an arbitrary stage. As a result, the mathematical formulation in terms of $[H^+]$ can be expressed as,

$$\begin{aligned} &[H^+] + 2(S_1 + S_2) \\ &\quad = \frac{K_w}{[H^+]} + \alpha_1(C_0 + S_1) + 2\alpha_2(C_0 + S_1) \end{aligned} \tag{4a}$$

$$\begin{aligned} \alpha_1 &= \frac{K_a[H^+]}{[H^+]^2 + K_a[H^+] + K_aK_b} \\ \alpha_2 &= \frac{K_aK_b}{[H^+]^2 + K_a[H^+] + K_aK_b} \end{aligned} \tag{4b}$$

$$\begin{aligned} &K_w = [H^+][OH^-] \quad K_a = \frac{[H^+][HCO_3^-]}{[H_2CO_3]} \\ &K_b = \frac{[H^+][CO_3^{2-}]}{[HCO_3^-]} \end{aligned} \tag{4c}$$

where, C_0 = concentration of dissolved carbon dioxide, S_1 = solubility of calcium carbonate, S_2 = solubility of calcium hydroxide, and K_w, K_a, K_b = equilibrium constant of concentration for each dissociation. Once the concentration of protons is obtained, each individual ionic concentration (Ca^{2+}, CO_3^{2-}, and so on) can be calculated.

Transport of carbon dioxide is considered for both the dissolved and gaseous carbon dioxide phases, which includes the effect of Knudsen diffusion and tortuosity of pores on diffusivity. Total flux of carbon dioxide for an arbitrary moisture history is expressed as,

$$J_{Co2} = -(D_{dCO_2}\nabla\rho_d + D_{gCO_2}\nabla\rho_g) \tag{5a}$$

$$\begin{aligned} D_{gCO_2} &= \frac{\phi \cdot D_0^g}{\Omega} \frac{(1-S)^n}{1 + l_m/2(r_m - t_m)} \\ D_{dCO_2} &= \frac{\phi S^n}{\Omega} D_0^d \end{aligned} \tag{5b}$$

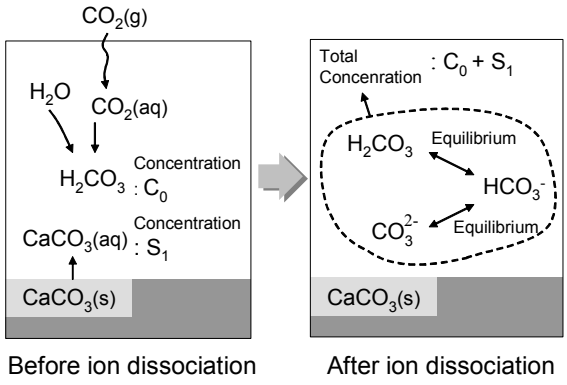

Fig.3 Mass balance and equilibrium conditions for carbonic acid.

where, D_{gCO2} = diffusion coefficient of gaseous CO_2 in a porous medium [m^2/s], and D_{dCO2} = diffusion coefficient of dissolved CO_2 in a porous medium [m^2/s]. In Eq. (5), the integral of the Knudsen number is simplified so that it can be easily put into practical computational use; r_m is the average radius of unsaturated pores, and t_m is the thickness of the adsorbed water layer in the pore whose radius is r_m. D_0^d is the diffusivity of dissolved CO_2 in pore water (=1.0×10^{-9} [m^2/s]) and D_0^g is the diffusivity of gaseous CO_2 in free atmosphere (=1.34×10^{-5} [m^2/s]) (Welty et al. 1969). l_m is the mean free path length of a molecule of gas. In Eq. (5), n is a parameter for representing the connectivity of the huge number of micropores, and it was initially proposed by Ishida and Maekawa (2001) based on the most simple assumption that the probability of unsaturated pores being connected to each other is proportional to the ratio of the volume in a cross section of each finite field. This assumption and an appropriate modeling of this connectivity will be further examined and elaborated in the following sections.

4. Changes in micropore structures due to carbonation

It has been reported that the micropore structure of cementitious material may change due to carbonation (JCI 1993, Houst and Wittmann 1994, Papadakis *et al*. 1991). In this work, the authors take into account changes in porosity caused by carbonation by applying a simplified model. It is assumed that the porosity distribution does not change, but that total porosity decreases as carbonation in progresses. Papadakis *et al*. (1991) showed experimentally that the reduction in porosity of fully carbonated concrete is dependent on the water-to-cement ratio. This fact also coincides well with the experimental results of Houst and Wittmann (1994) as well as Ngala and Page (1997). Based on these experimental results, the reduction of fully carbonated concrete/mortar can be empirically formulated (**Fig. 4**) as,

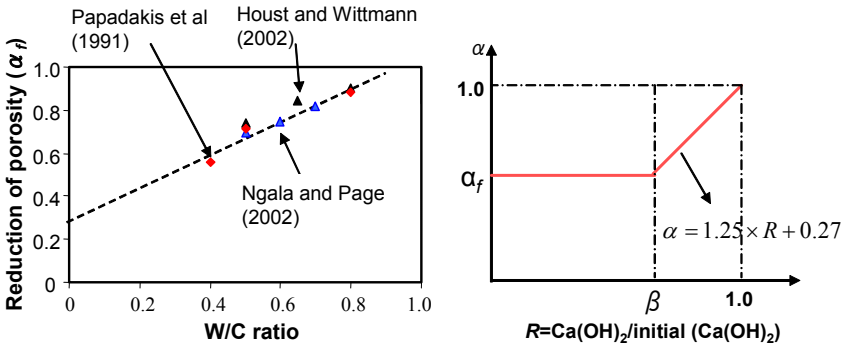

Fig.4 Influence of carbonation on porosity for different water-to-cement ratios.

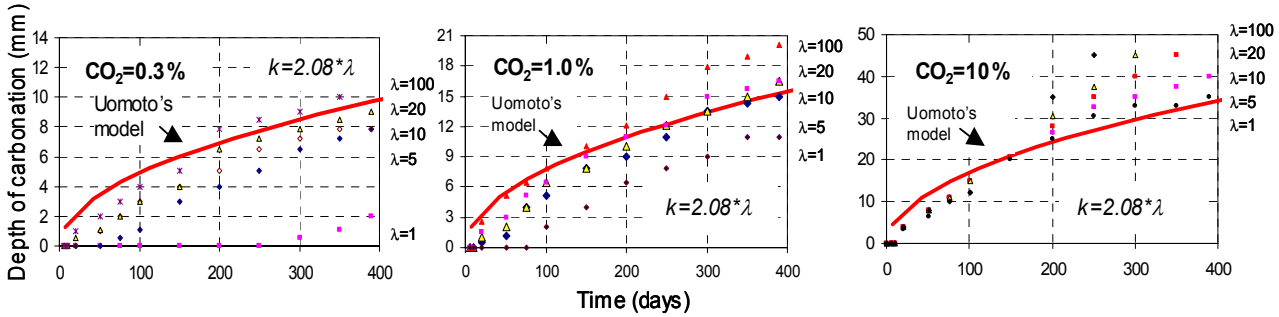

Fig. 5 Influence of reaction rate on carbonation depth (W/C=60%, 28 days submerged curing, RH=60%).

$$\alpha_f = 0.67 \cdot (w/c) + 0.27 \tag{6}$$

where, α_f is the reduction in porosity when a large amount of $Ca(OH)_2$ is consumed by carbonation (fully carbonated specimen). Due to the lack of experimental results for moderate level of carbonation (not fully carbonated), the porosity reduction factor for this level is simply modeled as a linear function of the remaining calcium hydroxide to its initial value which also coincides with the experimental work of Saeki *et al.* (1991) as initially modeled by Ishida and Maekawa (2001). The proposed bi-linear porosity reduction function is expressed as,

$$\phi' = \alpha\phi \quad \begin{matrix} \alpha = \alpha_f & (R \le \beta) \\ \alpha = 1.25 \cdot R + 0.27 & (\beta < R \le 1) \end{matrix} \tag{7}$$

where, ϕ = porosity before carbonation, ϕ' = porosity after carbonation, α = reduction parameter in porosity, R = degree of carbonation, which is expressed as the ratio of amount of remaining $Ca(OH)_2$ to the initial amount of $Ca(OH)_2$. A parameter β in Eq. (7) is formulated as,

$$\beta = 0.8\alpha_f + 0.2 \tag{8}$$

It has to be noted that the above porosity reduction function was mainly derived from the cases in which ordinary Portland cement was used. Past research has reported that the use of admixtures, such as blast furnace slag and fly ash, may cause a different change in the pore structure due to carbonation. This aspect remains a matter of future study for more precise prediction and wider applicability of the system.

5. Improved rate of reaction and CO_2 diffusivity – strong coupling with moisture profile

From a theoretical point of view, carbonation progress of cementitious materials is dependent on the rate of reaction and CO_2 diffusion as well as the nature of micropores, which are also affected by carbonation itself as shown in **Fig. 1**. The appropriate identification of these parameters is a key for improved simulation of carbonation phenomenon. A systematic parametric study with support of experimental events is used to simply formulate these parameters.

Carbonation processes are not analogous in the case of accelerated tests in a short period and in the case of natural carbonation under long-term exposure to natural atmosphere. This difference is attributed to moisture distribution under different drying periods as well as changes in micropore structures that may depend on CO_2 concentration. **Figure 5** shows numerical results of carbonation depth under different CO_2 concentrations (0.3%, 1%, and 10%). The influence of the reaction rate on carbonation progress is examined by changing reaction rate coefficient k in Eq. (2). In the original model that was verified mainly with accelerated tests, a value of 2.08 [l/mol.sec] was used, whereas in this study

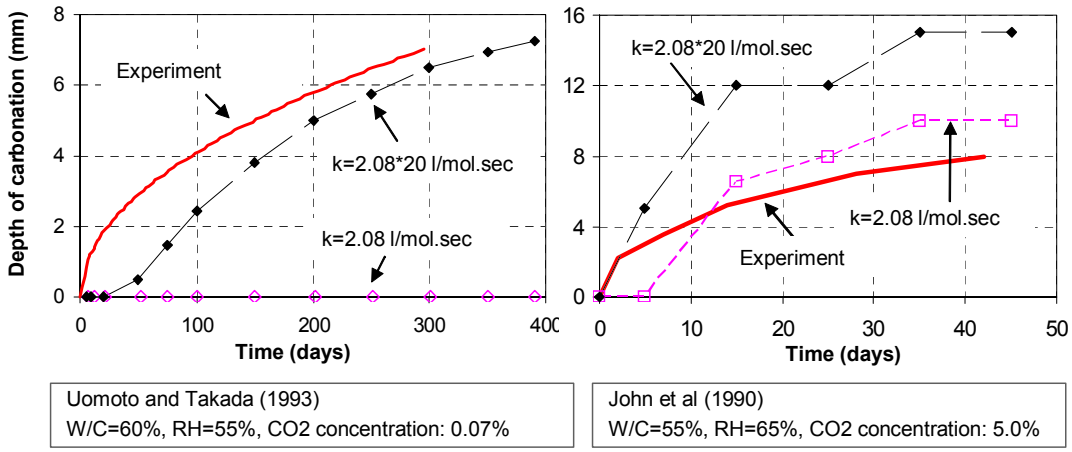

Fig. 6 Influence of reaction rate on predicted carbonation depth.

five cases were studied in order to find an improved parameter for a wide range of CO_2 concentrations. The connectivity of micropore structures is assumed by setting parameter n equal to 4 in Eq. (4) as initially proposed by Ishida and Maekawa (2001) for lower relative humidity conditions. The results are compared with an empirical equation proposed by Uomoto and Takada (1993), which covers experimental results both for accelerated and natural carbonation tests.

As could easily be expected, higher values of the reaction rate coefficient result in higher carbonation depths. However, this influence is more significant in the case of low CO_2 concentration. Increases in the carbonation rate coefficient greatly affect the depth of carbonation in the case of low CO_2 concentration. It is also shown that, in a short period of carbonation, higher values give better predictions for moderate/high CO_2 concentration.

This influence can also be seen in numerical prediction of experimental work of Uomoto and Takada (1993) and John *et al*. (1990), as shown in **Fig. 6**. The analytical results for two different values of the reaction rate coefficient (appropriate for low CO_2 concentration and accelerated cases) are shown in this figure. It is obvious that, on the basis of the above assumptions, even though analytical results for the low reaction rate coefficient agree well with the accelerated carbonation test, it cannot show the progress of carbonation in low CO_2 concentration. The comparison of analytical results with experiment of John *et al* (1990), which is an accelerated carbonation test for a period of only 40 days, shows that the carbonation rate is too high in the analysis using the reaction rate coefficient that is appropriate for natural carbonation.

Let us consider the pore moisture distribution in the specimen. When we deal with a short testing period (such as an accelerated carbonation test), the relative humidity of pores is still large in a little far region from the surface of the specimen. This high relative humidity, in reality, significantly prevents the penetration of carbon dioxide into the specimen, which should be carefully considered in the numerical modeling. Saturated pores block the migration of gaseous carbon dioxide, in other words, the diffusivity of CO_2 declines as the relative humidity of pores increases. Such an influence is of particular importance for an accurate prediction of the carbonation process in accelerated carbonation tests, where the depth of carbonation develops into a large relative humidity domain. **Figure 7** shows the computed moisture distribution along the depth of examined specimen subjected to different CO_2 concentrations (0.07%, 1%, 10%) at the time when the depth of carbonation is the same (5 cm). It can be seen that at a low CO_2 concentration, the specimen is completely dried after a long-term carbonation process. However, in accelerated carbonation tests, the value of RH is still large

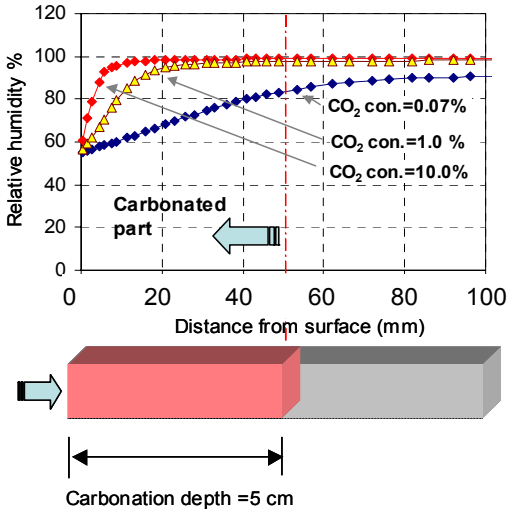

Fig. 7 Computed moisture distribution along the specimen under different CO_2 concentrations when the depth of carbonation is 5 cm (RH at boundary = 55%, W/C=60%).

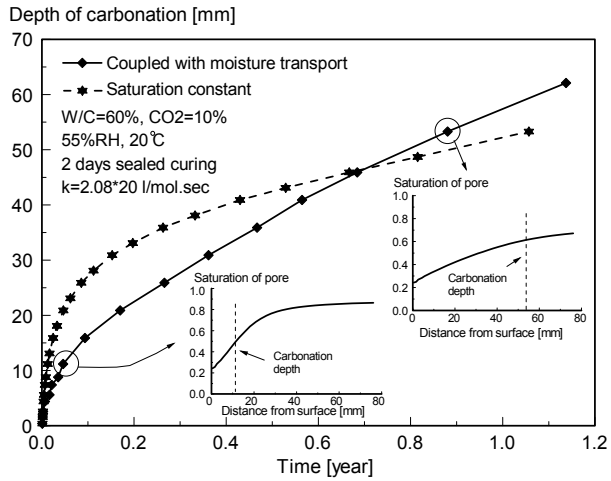

Fig.8a Effect of moisture distribution on carbonation progress (CO_2=10%).

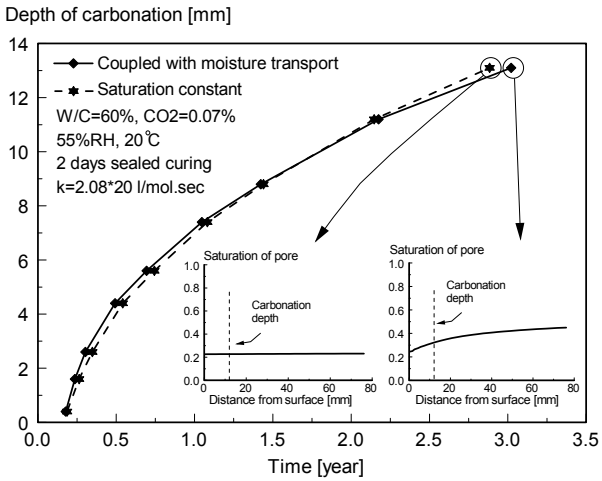

Fig.8b Effect of moisture distribution on carbonation progress (CO_2=0.07%).

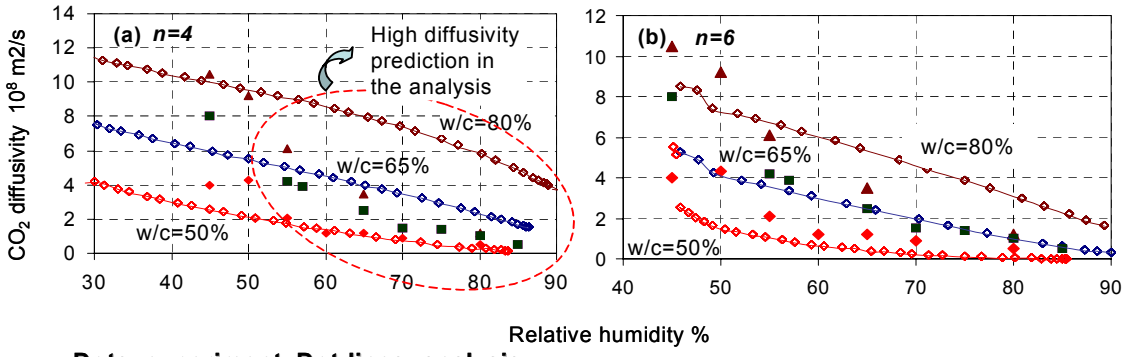

Fig.9 Comparison of experiment and analytical prediction using two different valued of connectivity parameter (n=4, 6).

even close to the surface of the specimen.

Figure 8 is an example that shows the effect of moisture distribution on the progress of carbonation. For comparison, two cases were analyzed: one is a coupled analysis with moisture transport, and the other assumes that the pore structures in all domains have the same saturation. It is shown that the progress of carbonation under a high CO_2 concentration is highly dependent on the moisture distribution, whereas no significant difference is observed in the case of atmospheric concentration. As shown in **Fig. 8a**, there is a large moisture gradient inside concrete just after exposure to drying, which leads to a delay in carbonation at the initial stage. After one year, the analysis coupled with moisture shows a larger depth of carbonation, since much of the condensed liquid water retains in the carbonated domain, which leads to higher rate of the carbonation reaction. It should be noted here that, in the analysis, moisture release caused by the decomposition of hydrates during carbonation was not taken into account for the sake of simplicity. Therefore, especially in the accelerated carbonation test shown in **Fig. 8**, the analytical result may still underestimate the coupling effect of moisture distribution and carbonation progress. In other words, the amount of condensed liquid water in reality may be larger than the calculated results. This aspect will be studied in future by including the contribution of the released water into the sink term of the mass balance equation of moisture.

The above discussions have clarified that interdependence between CO_2 diffusivity and moisture distribution should be taken into account for the accurate prediction of carbonation. First, a sensitivity analysis was carried out in order to obtain a more appropriate value for CO_2 diffusivity especially under high relative humidity. Papadakis *et al* (1991) experimentally investigated the influence of RH on CO_2 diffusivity. On the basis of their experiment, herein the connectivity parameter (n in Eq. (4)) is simply re-assumed to be equal to 6, which is the most appropriate value for simulation of CO_2 diffusivity under large relative humidity, as shown in **Fig. 9**. The original assumption of Ishida and Maekawa (2001) (n=4), as shown in **Fig. 9**, has a good agreement for low relative humidity conditions, but it is overestimated for large relative humidity cases. The appropriate modeling of carbon dioxide diffusivity for a wide range of relative humidity conditions is herein addressed for further study, but it should be noted that

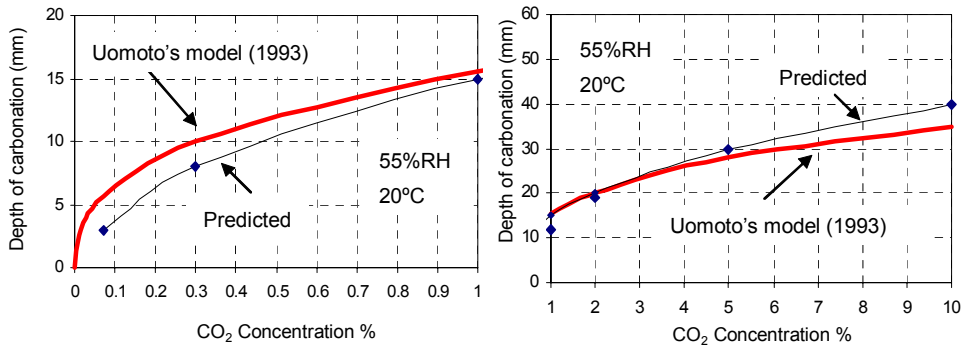

Fig. 10 Numerical prediction of influence of CO_2 concentration on depth of carbonation.

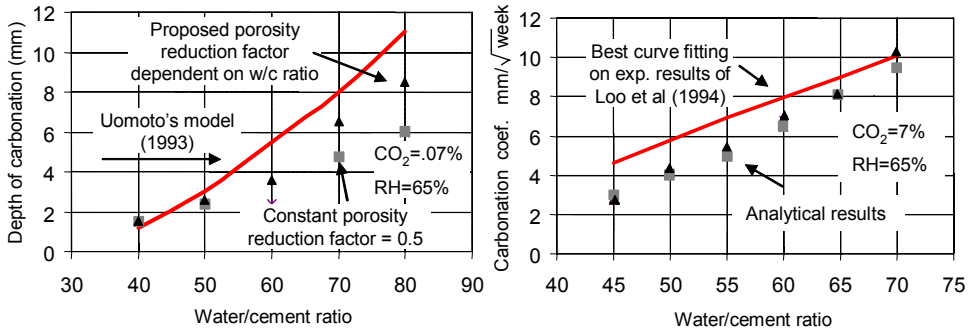

Fig. 11 Numerical prediction of influence of W/C ratio on depth of carbonation.

the influence of such an effect is much higher in cases of accelerated carbonation test, in which the depth of carbonation developed into a large relative humidity domain. The analytical results using the modified connectivity parameter (n=6) and the high reaction rate coefficient (k=2.08×20[l/mol.sec]), which is simply proposed for low CO_2 concentration, are shown in **Fig. 10**. It can be seen that appropriate modeling of CO_2 diffusivity as well as the reaction rate coefficient greatly improves the simulation of the carbonation process in both accelerated and natural carbonation cases.

Figure 11 shows the influence of the water-to-cement ratio on the numerical prediction of carbonation depth and its comparison with Uomoto's model (Uomoto and Takada 1993) and the experiment of Loo *et al*. (1994). The influence of the porosity reduction factor was also examined as shown in **Fig. 11**. It can be seen that the proposed porosity reduction factor can effectively improve the prediction of carbonation depth for higher water-to-cement ratio cases.

6. Carbonation process under accelerated and normal environment - Is analogy between two conditions always assured?

An accelerated carbonation test has been often used to assess the durability performance of materials, since it gives useful information on long-term performances at short intervals of time. In general, it has been assumed that the carbonation process would be analogous to that under a real environment. However, there is no consensus on how much the accelerated test will shorten the real time-scale from a quantitative viewpoint, or whether it will correctly simulate the trend of the material behavior exposed to the natural environment from a qualitative point of view. Against these backgrounds, the analytical model discussed in the previous section is used to investigate similarities or differences in the depth of carbonation under high and low CO_2 concentrations.

Figure 12 shows the carbonation processes of concrete exposed to CO_2 concentrations of 10% (**Fig. 12a**) and 0.07% (**Fig. 12b**) at constant temperature and relative humidity (20°C, 55%RH) after 2 days of sealed curing. Three different water-to-cement ratios, W/C=40%, 60%, and 80%, were specified in the analysis. In these computations, only ordinary Portland cement was used as a binder. Regardless of the ambient concentrations, it was shown that the depth of carbonation increases with higher water-to-cement ratio. For the purpose of direct quantitative comparison between two cases, carbonation rate coefficients α_c were obtained as shown in **Fig. 12** and **Table 1**. The coefficient is defined as,

$$y_d = \alpha_c \sqrt{t} \tag{9}$$

Table 1 Calculated carbonation rate coefficient for different concentrations of ambient CO_2.

W/C	Carbonation rate coefficient α_c^1 [mm/$\sqrt{\text{year}}$] (CO_2=10%)	Carbonation rate coefficient α_c^2 [mm/$\sqrt{\text{year}}$] (CO_2=0.07%)	α_c^1/α_c^2
80%	79.1	10.8	7.32
60%	51.2	6.8	7.53
40%	23.9	3.0	7.97

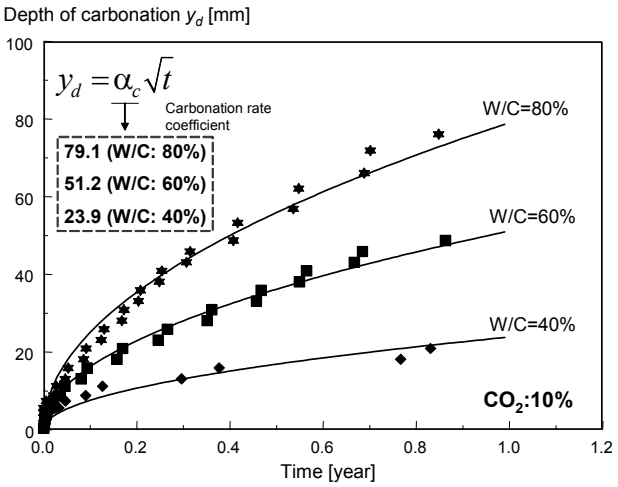

Fig. 12a Prediction of carbonation phenomena for difdifferent W/C (CO_2=10%).

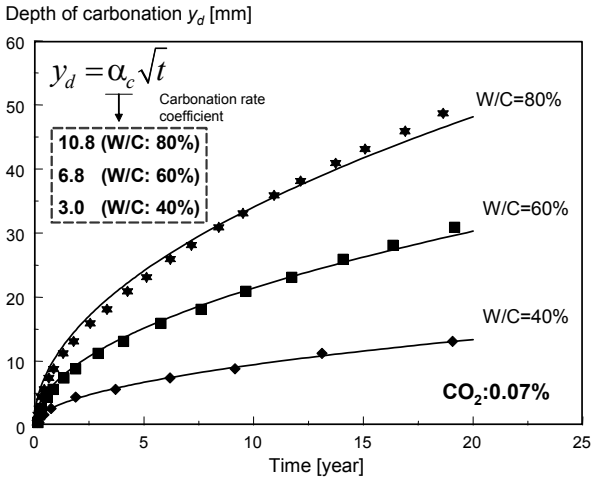

Fig. 12b Prediction of carbonation phenomena for difdifferent W/C (CO_2=0.07%).

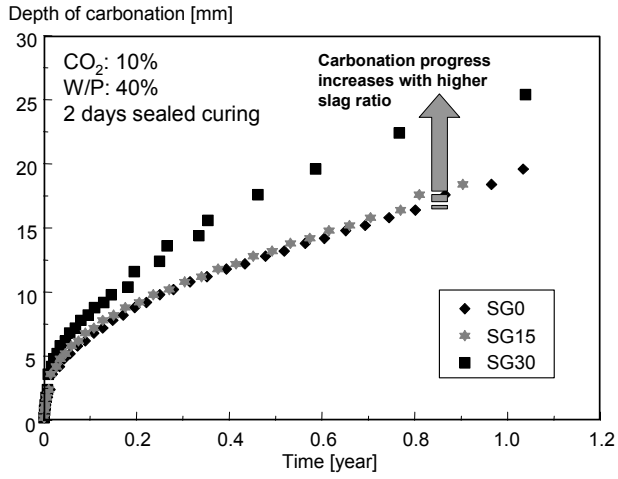

Fig. 13a Carbonation progress of concrete for various amount of (CO_2=10%).

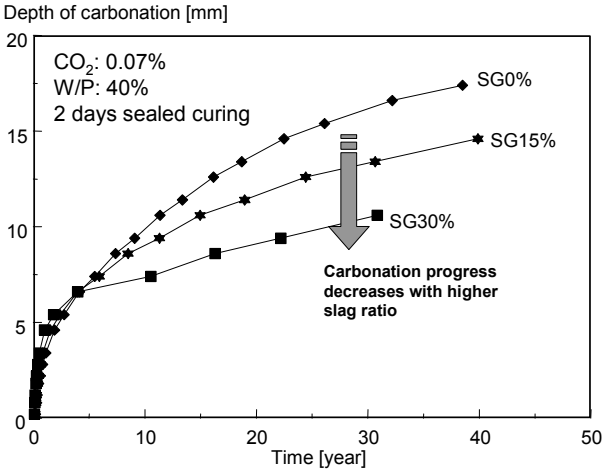

Fig. 13b Carbonation progress of concrete for various amount of blast furnace slag (CO_2=0.07%).

where, y_d = depth of carbonation [mm], and t = exposure time. According to Eq. (9), a regression analysis was carried out to obtain α_c based on the computational results. **Table 1** shows the carbonation rate coefficients, α_c^1 for CO_2 = 10%, α_c^2 for CO_2 = 0.07%, and the ratio of α_c^1 to α_c^2 which allows us to convert the time scale in accelerated environments into the time scale under normal condition. As shown in the table, roughly speaking, the ratios have almost the same values of about 7 to 8. It must also be noted that the ratio increases slightly in the case of a lower water-to-cement ratio, which means that the accelerated test underestimates the resistance to car-

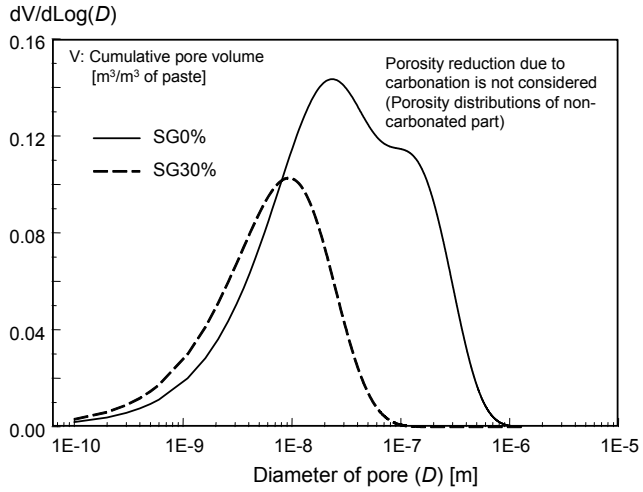

Fig. 14 Distribution of micro pore structural volume For different.

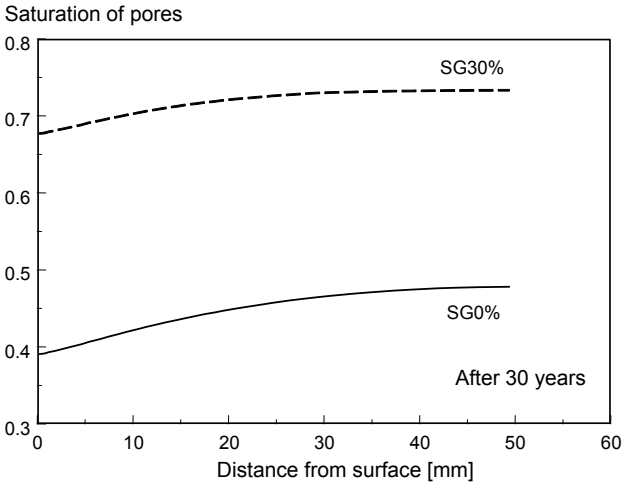

Fig. 15 Distribution of saturation in micro pore structure after 30 BFS content years.

bonation of lower W/C concrete.

Next, a sensitivity simulation was carried out to demonstrate behaviors when using an admixture. Blast furnace slag was mixed into concrete at three different ratios to the total weight of powder (SG0: 0%, SG15: 15%, and SG30: 30%). A constant water-to-powder ratio was given (W/P = 40%). Numerical results are shown in **Fig. 13**. Under the accelerated condition, in the case of SG30, carbonation progresses rapidly compared with SG0 and SG15. On the contrary, the calculated depth of carbonation under the low CO_2 concentration shows the opposite trend unlike the previous analysis. As the amount of slag increases, the carbonation rate decreases.

When blast furnace slag is mixed into concrete, a trade-off of strongly coupled effects can be expected: an increment in the consumption of $Ca(OH)_2$ as a source of alkalinity due to the reaction and the dense micropore structure that leads to low CO_2 diffusivity. **Figure 14** shows the calculated pore-structure distribution for SG0 and SG30. In the case of slag in use, total porosity decreases and the pore structure becomes finer. In such a denser micropore structure, from a thermodynamic point of view, saturation of the pore maintains a higher value compared with the SG0 case, even though relative humidity inside the pore is same. This theoretical inference is supported by **Fig. 15**, i.e., the micropore structure in the SG30 case is highly saturated. **Figure 16** shows the distribution of calcium hydroxide for both cases. It can be observed that, due to the reaction of blast furnace slag, the amount of $Ca(OH)_2$ is reduced to almost half the quantity of the SG0 case.

Based on these results, let us discuss a mechanism that causes a contradictory trend to that obtained by the analysis. In the case of accelerated testing, the amount of calcium hydroxide will mainly control the rate of carbonation; A high CO_2 concentration in the surrounding environment brings a large potential gradient between outside and inside concrete, then it allows a larger amount of gaseous CO_2 to diffuse into a specimen, even though inside the pores maintain high saturation. Consequently, in such a case, the amount of migrating CO_2 would be enough to consume reduced $Ca(OH)_2$ in slag concrete. On the other hand, under a natural ambient climate, the rate of carbonation depends on the nature of the micropore structure, since only a small amount of carbon dioxide is available for the reaction. In other words, the dense micropore structure and resulting low diffusivity will overcome the disadvantage caused by the small amount of calcium hydroxide as the source of alkalinity. Here, it has to be noted that this opposite trend may not be observed in higher water-to-cement ratio concrete (such as W/P 50% to 60%), since such concrete still has high diffusivity even though blast furnace slag is used. At any rate, a point to be emphasized through this study is that accelerated testing does not always yield a consistent trend with natural carbonation

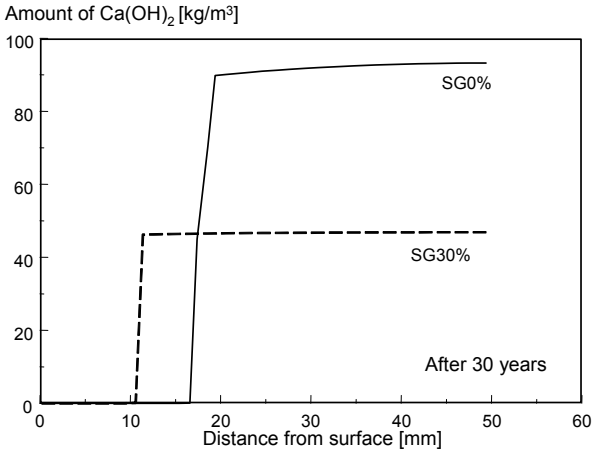

Fig. 16 Distribution of remaining calcium hydroxide in concrete pores after 30 years

process, and in such a case, numerical simulation tools can support appropriate material and durability designs.

7. Conclusions

Influential parameters on prediction of carbonation depth involving reaction rate, carbon dioxide diffusivity and change of micro pore structures caused by carbonation are numerically discussed through a parametric study and comparison with available experimental results. Appropriate parameters for material modeling on the basis of already developed computational scheme were successfully identified. It is shown that the reaction rate coefficient has a great influence on the evolution of carbonation, especially in ambient weathering conditions. However, the most important factor that affects the carbonation depth under accelerated environmental actions is carbon dioxide diffusivity. Moisture saturation in short-term carbonation tests largely control/prevent the evolution of carbonation. In addition, through sensitivity analyses, it has been clarified that different moisture profile may sometimes bring the opposite trend of the carbonation reaction under low and high CO^2 concentrations. Accordingly, this point should be considered carefully when carrying out material design and/or durability assessment based on an accelerated test.

Acknowledgement

This study was supported by grant-in-aid for scientific research No.15686019 from MEXT, and the program for promoting fundamental transport technology research from Japan Railway Construction, Transport and Technology Agency (JRTT).

References

Houst, Y. F. and Wittmann, F. H. (1994). "Influence of porosity and water content on the diffusivity of CO_2 and O_2 through hydrated cement paste" *Cement and Concrete Research*, 24 (6), 1165-1176.

Ishida, T. and Maekawa, K. (2001). "Modeling of pH profile in pore water based on mass transport and chemical equilibrium theory" *Concrete Library of JSCE*, 37, 131-146.

JCI (1993). "The report of JCI Committee on Carbonation" *Japan Concrete Institute*, (in Japanese).

John, J., Hirai, K. and Mihashi, H. (1990). "Influence of environmental moisture and temperature on carbonation of mortar" *Concrete Research and Technology*, JCI, 1 (1), 85-94 (in Japanese).

Loo, Y. H., Chin, M. S., Tam, C. T. and Ong, K. C. G. (1994). "A carbonation prediction model for accelerated carbonation testing of concrete" *Magazine of Concrete Research*, 46 (168), 191-200.

Maekawa, K., Ishida, T. and Kishi, T. (2003). "Multi-scale modeling of concrete performance" *Journal of Advanced Concrete Technology*, Vol.1, No.2, 91-126.

Maekawa, K., Chaube, R. P. and Kishi, T. (1999). "*Modelling of Concrete Performance*" London: E&FN SPON.

Maekawa, K. and Ishida, T. (2002). "Modeling of structural performances under coupled environmental and weather actions" *Materials and Structures*, 35, 591-602.

Ngala, V. T. and Page, C. L. (1997). "Effects of carbonation on pore structure and diffusion properties of hydrated cement pastes" *Cement and Concrete Research*, 27 (7), 995-1007.

Papadakis, V. G., Vayenas, G. G. and Fardis, M. N. (1991). "Fundamental modeling and experimental investigation of concrete carbonation" *ACI Material journal*, 88 (4), 363-373.

Saeki, T., Ohga, H. and Nagataki, S. (1991). "Mechanism of carbonation and predicting of carbonation process of concrete", *Concrete Library of JSCE*, 17, 23-36.

Uomoto, T. and Takada, Y. (1993). "Factors affecting concrete carbonation ratio", *Concrete library of JSCE*, 21, 31-44.

Welty, J. R., Wicks, C. E. and Wilson, R. E. (1969). "*Fundamentals of momentum, heat, and mass transfer*" New York: John Wiley & Sons, Inc.